Geomechanics and Engineering, *Vol. 41, No. 1 (2025) 33-41*
https://doi.org/10.12989/gae.2025.41.1.033

Enhancing bearing capacity through optimal pile group spacing and arching effect

Chanhee Kim[1a], Seongjin Kil[2b], Jaewon Kim[2c], Kabboo Kim[3d], Younguk Kim[2e] and Junho Moon*[2]

[1]*Offshore Wind Power Depart., BANDI Consultants Co.,Ltd., Republic of Korea*
[2]*Department of Civil and Environmental Engineering, Myongji Univ., Republic of Korea*
[3]*Busiddol Inc., Republic of Korea*

(*Received December 7, 2024, Revised February 26, 2025, Accepted March 5, 2025*)

Abstract. This study investigates the effect of pile spacing on the bearing capacity of group piles and proposes optimal spacing to enhance design efficiency. The theoretical analysis, based on Terzaghi's failure mode and the arching effect, evaluates the influence of spacing adjustments on bearing capacity improvement. Laboratory model tests were conducted to experimentally validate the theoretical findings, comparing pile capacities under various spacing conditions. The results reveal that arching effects become significant when the spacing ratio exceeds 1.7, leading to a substantial increase in bearing capacity. This research proposes an optimal spacing range to supplement current design standards and provides foundational data for efficient pile design.

Keywords: arching effect; group pile efficiency; pile spacing; soil bearing capacity; terzaghi failure

1. Introduction

Foundation structures play a critical role in transferring loads from superstructures to the ground in a stable manner, thereby ensuring the stability and durability of the overall structure (Józefiak *et al*. 2015). To prevent excessive deformation or failure and to guarantee structural stability, it is essential to design foundations that evenly distribute loads to the ground based on site-specific soil characteristics.

The selection of foundation types is optimized by considering various factors, such as the distribution of soil layers, ground conditions, constructability, superstructure type, and environmental influences (Khanmohanmmadi *et al*. 2022). For instance, soil strength, groundwater levels, and the size and shape of the superstructure significantly impact the choice of foundation. Particularly in cases where non-uniform soil distribution is expected, foundations capable of adapting to multiple soil layers should be considered. Furthermore, construction conditions and environmental constraints also play a vital role in the selection process.

Pile foundations are predominantly used in soft ground or where the surface soil lacks sufficient bearing capacity to transfer loads directly to deeper, more stable layers. These foundations are advantageous for preventing settlement and ensuring ground stability by transferring loads securely to deep strata (Alsanabandi *et al*. 2023). Pile foundations are especially effective under complex ground conditions, such as soft soils, high groundwater levels, or reclaimed land, where they provide high bearing capacity.

Pile spacing is a crucial factor in pile foundation design, with minimum spacing guidelines specified in design standards. If the spacing is too narrow, stress overlap between adjacent piles can lead to a reduction in bearing capacity, known as the "group pile effect." For instance, the Foundation Design Standards of Korea require a minimum spacing of 2.5 times the pile diameter, a criterion similarly adopted by the American Association of State Highway and Transportation Officials (AASHTO). In contrast, EUROCODE 7 (EN 1997-1: Geotechnical Design) does not prescribe specific spacing requirements, instead offering flexibility for designers to adjust spacing as needed.

Recently, various studies have evaluated the impact of pile spacing adjustments on bearing capacity and design efficiency. Kumar *et al*. (2024) investigated the dynamic behavior of group piles under multi-directional loading, while Nguyen *et al*. (2023) proposed methods to reduce the moments and displacements of sheet piles. Lv *et al*. (2023) examined the effects of load magnitude and cushion thickness on horizontal bearing mechanisms, and Yun and Han (2023) evaluated the dynamic behavior of piles installed on rubble-mound-reinforced slopes. Additionally, Zhou and Tokimatsu (2018) utilized 3D FEM to study group effects in various group pile configurations, while Nasrollahzadeh and Hataf (2019) conducted experimental and numerical analyses of tapered and cylindrical group piles to quantify the impact of pile numbers and spacing on group effects. These studies collectively highlight the complexity of pile behavior, which is influenced by

*Corresponding author, Research Professor
E-mail: jhmoon@mju.ac.kr
[a]Assistant Engineer
[b]Master's Degree Student
[c]Master's Degree Student
[d]CEO (Chief Executive Officer)
[e]Professor

Copyright © 2025 Techno-Press, Ltd.

ISSN: 2005-307X (Print), 2092-6219 (Online)

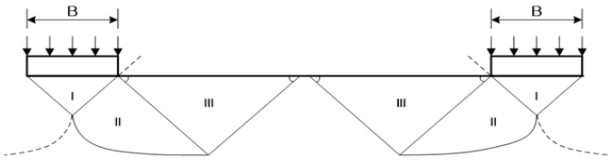

(a) Loose Sand Failure Mode

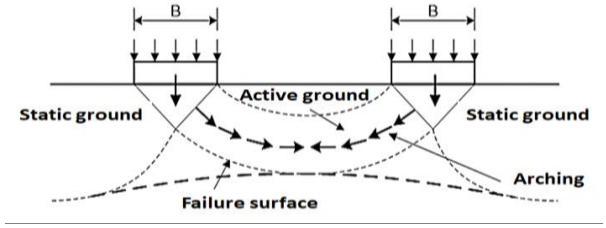

(b) Dense Sand Failure Mode

Fig. 1 Arching Effect in Actual Ground

multiple factors such as ground conditions, pile spacing, installation angles, pile arrangement, and the presence of pile caps.

This study applies the arching effect and Terzaghi failure mode to theoretically determine optimal pile spacing and analyzes the ultimate bearing capacity and efficiency of group piles through load tests. By examining the overall behavior of group piles and verifying the contribution of the arching effect at pile tips to increased bearing capacity, the study aims to propose an optimal pile spacing range that can supplement existing design standards.

2. Arching effect

The arching effect refers to the phenomenon where particles interact to form a stable arch, redistributing forces and transmitting loads to adjacent soil, thereby maintaining overall stability (Lian *et al*. 2015, He *et al*. 2017, Hong and Hong, 2017, Xu *et al*. 2023). In actual ground conditions, when foundations are installed in close proximity, the arching effect causes earth pressure at certain points to be transferred to adjacent stable soil (Fig. 1). For instance, when some soil particles in the ground yield due to increased earth pressure, part of the self-weight of surrounding soil particles shifts toward more stable particles. This interaction generates shear resistance at the contact area, reducing the earth pressure at the yielding point while increasing it in the stable zone. Furthermore, soil particles undergoing excessive displacement redistribute stress to adjacent particles, reducing the stress on the displaced particles. This arching effect is more pronounced in sandy soils than in silts or clays and becomes stronger as soil density increases.

In the case of pile foundations, the arching effect at the pile tip can be explained by Terzaghi's failure mode. When group piles are arranged at equal spacing, the shear failure planes of adjacent piles overlap, suppressing each other's shear failure and thereby increasing bearing capacity (Fig. 2). In this process, the shear forces between adjacent piles transform into passive earth pressure, acting in a wedge shape. At the lower ends of adjacent pile tips, these soil

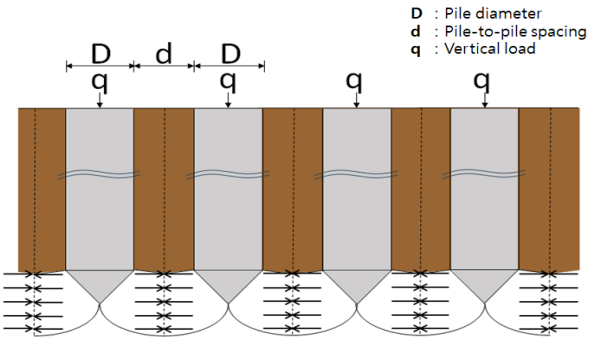

Fig. 2 Arching Effect Induced by Shear Interaction in Group Piles

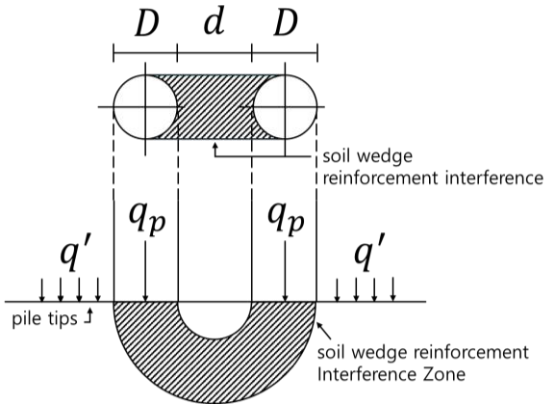

Fig. 3 Soil Wedge Reinforcement Interference Between Group Piles

wedges interlock, activating the arching effect. By adjusting the pile spacing to intentionally amplify this arching effect at the pile tips, it is possible to achieve higher bearing capacity than that of conventional group piles.

3. Optimal pile spacing

When group piles are installed, the ground volume expands by the volume of the piles (V), inducing stress in the surrounding soil (Zhang *et al*. 2019, Cai *et al*. 2023). The soil wedge reinforcement interference theory explains the stress behavior caused by this volumetric expansion and suggests that reinforcement effects can occur through the interaction of voids between adjacent piles (Fig. 3). In particular, when adjacent piles are installed in close proximity, the voids formed around each pile overlap, creating an interaction effect that increases bearing capacity.

At the pile tip, the arching effect and soil wedge reinforcement interference act simultaneously, significantly influencing the bearing capacity. Based on theoretical backgrounds, this study aims to determine the optimal spacing between piles to maximize bearing capacity.

3.1 The first theory

The first theory assumes that for the soil wedge at the

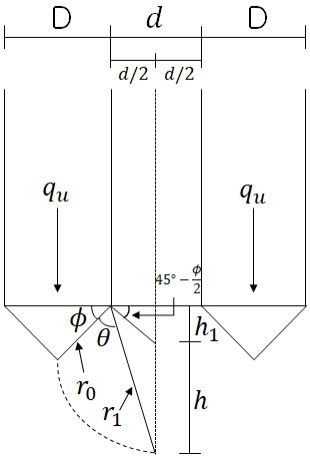

Fig. 4 Shear Failure Patterns at Pile Tips (1st theory)

pile tip to interact with the soil wedge of an adjacent pile and generate reinforcement effects, the interference height (h) must be equal to the pile diameter (D) (Fig. 4).

$$h = D \tag{1}$$

When the stress acting on the soil at the pile tip exceeds the soil's shear strength, a shear failure plane is formed. The trajectory of this shear failure plane is expressed by Eq. (2). The exponential function in this equation reflects the rotation and nonlinear deformation characteristics of the failure plane.

$$r_1 = r_0 \cdot e^{\theta \cdot \tan\varphi} \tag{2}$$

The relationship between the pile diameter (D) and the slope of the soil wedge (r_0) can be expressed by Eq. (3).

$$D = 2r_0 \cdot \cos\varphi \tag{3}$$

Similarly, the relationship between the pile spacing (d) and the shear failure plane can be expressed by Eq. (4).

$$d = 2r_1 \cdot \cos\big(\pi - (\varphi + \theta)\big) \tag{4}$$

The total height from the pile tip to the center of the pile spacing, including the soil wedge height (h_1+h), as well as the individual component heights (h_1), can be derived using Eqs. (5) and (6), resulting in Eq. (7). Finally, the spacing ratio (m) between piles can be expressed as Eq. (8).

$$h_1 + h = r_1 \cdot \sin\big(\pi - (\varphi + \theta)\big) \tag{5}$$

$$h_1 = r_1 \cdot \cos\big(\pi - (\varphi + \theta)\big) \cdot \tan\left(45° - \frac{\varphi}{2}\right) \tag{6}$$

$$h = r_0 \cdot e^{\theta \cdot \tan\varphi} \cdot \Big[\sin\big(\pi - (\varphi + \theta)\big) - \cos\big(\pi - (\varphi + \theta)\big) \cdot \tan\left(45° - \frac{\varphi}{2}\right)\Big] \tag{7}$$

$$m = \frac{d+D}{h} = \frac{d+D}{D} = \frac{\cos\big(\pi - (\varphi + \theta)\big)}{\Big[\sin\big(\pi - (\varphi + \theta)\big) - \cos\big(\pi - (\varphi + \theta)\big) \cdot \tan\left(45° - \frac{\varphi}{2}\right)\Big]} + 1 \tag{8}$$

Table 1 Optimal Pile Spacing Based on First Theory

φ(°)	θ(°)	m=(d+D)/D
30	60 < θ < 75	0 < m < 1.6339
31	59 < θ < 78.5	0 < m < 1.8856
32	58 < θ < 81	0 < m < 2.1101
33	57 < θ < 83	0 < m <2.3268
34	56 < θ < 85.5	0 < m < 2.6184
35	55 < θ < 87.5	0 < m < 2.9064

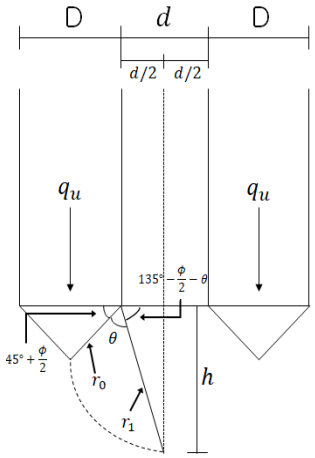

Fig. 5 Shear Failure Patterns at Pile Tips (2nd theory)

Eq. (8) is a function of φ and θ that satisfies the condition h=D. By substituting various combinations of φ and θ into this equation, the range of pile spacing ratios can be determined. Table 1 presents the calculated values of θ and m for different shear resistance angles (φ).

3.2 The second theory

Unlike the first theory, the second theory assumes that the overlapping effect is optimized when the height of the soil wedge formation, relative to the pile diameter (h/D), reaches its maximum (Fig. 5). To ensure that the vertical load from adjacent piles is transferred over the largest possible area through the shear failure planes of the subsoil beneath the pile tip, the spacing distance must be calculated to achieve the maximum height (h) where the two shear failure planes fully interact.

Based on the schematic shown in Fig. 5 and using a geometric approach, the height (h) of the soil wedge formation from the pile tip to the center of the pile spacing, the pile diameter (D), and the pile spacing (d) can be expressed by Eqs. (9)-(11).

$$h = r_1 \cdot \sin\left(135° - \frac{\varphi}{2} - \theta\right) \tag{9}$$

$$D = 2r_0 \cdot \cos\left(45° + \frac{\varphi}{2}\right) \tag{10}$$

$$d = 2r_1 \cdot \cos\left(135° - \frac{\varphi}{2} - \theta\right) \tag{11}$$

Table 2 Optimal Pile Spacing Based on Second Theory

$\varphi(^\circ)$	$\theta(^\circ)$	h/D	m=(d+D)/D
30	60	1.585	2.831
31	60	1.641	2.934
32	61	1.701	3.125
33	61	1.764	3.248
34	62	1.832	3.471
35	62	1.904	3.617

Additionally, Eq. (12) provides a functional relationship between φ and θ, which allows for the calculation of the height-to-diameter ratio (h/D) under various combinations of φ and θ. When h/D reaches its maximum, Eq. (13) can be used to determine the pile spacing ratio that generates the optimal overlapping effect. The results are summarized in Table 2.

$$\frac{h}{D} = \frac{e^{\theta \cdot \tan\varphi} \cdot \sin\left(135^\circ - \frac{\varphi}{2} - \theta\right)}{2 \cdot \cos\left(45^\circ + \frac{\varphi}{2}\right)} \quad (12)$$

$$m = \frac{d+D}{D} = \frac{e^{\theta \cdot \tan\varphi} \cdot \cos\left(135^\circ - \frac{\varphi}{2} - \theta\right)}{\cos\left(45^\circ + \frac{\varphi}{2}\right)} + 1 \quad (13)$$

In this study, the minimum pile spacing is set at 2.5D or less, in accordance with domestic design standards. Subsequently, a laboratory model test is planned based on the first theory to evaluate the changes in vertical bearing capacity.

4. Laboratory model tests

4.1 Material property tests

The sample used in this experiment was Jumunjin standard sand, and material property tests were conducted following applicable standards to determine its basic properties. Based on these results, the relative density of the model ground, the arrangement of group piles, and their spacing were determined, and subsequent pile loading tests were carried out.

Sand pluviation test

Maintaining consistent relative density during the preparation of the model ground is crucial. The experimental setup for the sand pluviation test was planned with reference to the model studies of Abdollahi and Bolouri Bazaz (2017) and Dastpak *et al*. (2021). Key factors affecting relative density include drop height, sand discharge rate, and device movement speed. Among these, the drop height serves as a variable for controlling potential energy, with an increase in height generally leading to higher relative density. However, when particles reach their terminal velocity, the relative density ceases to increase significantly.

Table 3 Drop Height vs. Relative Density in Sand Pluviation

	A	B	C	D	E	F
H(m)	0.22	0.27	0.32	0.37	0.42	0.47
γ_d(kN/m^3)	15.5	15.6	15.8	15.9	15.9	15.9
D_r(%)	64.1	65.9	71.1	72.8	72.8	72.8

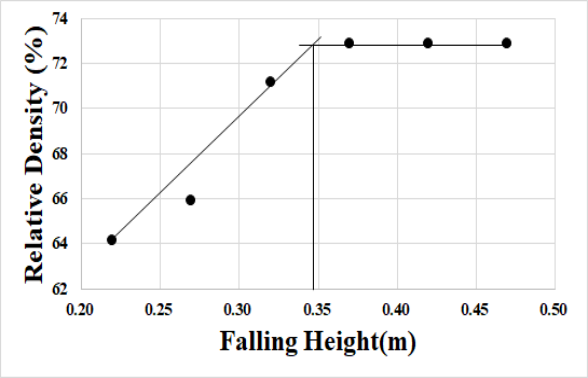

Fig. 6 Drop Height vs. Relative Density in Sand Pluviation

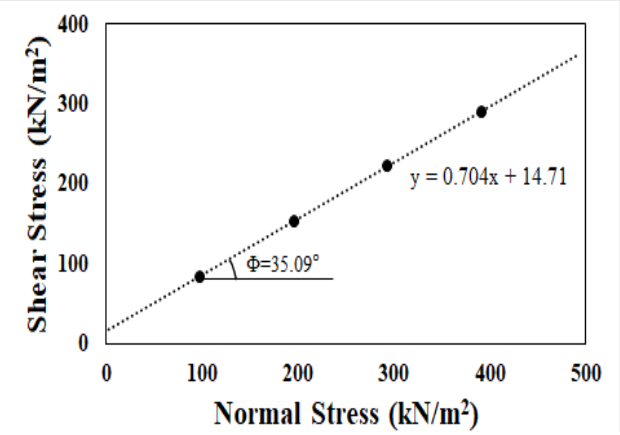

Fig. 7 Normal Stress vs. Shear Stress in Direct Shear Test

In this section, soil compaction was controlled by adjusting the drop height, and the corresponding variations in dry unit weight were analyzed. A key parameter for assessing the compaction of sandy soil using the sand pluviation method is its relative density, which represents the degree of compactness or looseness of granular soils, as defined in Eq. (14). The maximum and minimum dry unit weights of the sample were determined to be 16.9 kN/m³ and 13.6 kN/m³, respectively. By applying the dry unit weight obtained from the drop height test to Eq. (14), the relative density values presented in Table 3 were calculated.

$$D_r = \left[\frac{\gamma_{d.max}}{\gamma_d}\right]\left[\frac{\gamma_d - \gamma_{d.min}}{\gamma_{d.max} - \gamma_{d.min}}\right] \times 100(\%) \quad (14)$$

Fig. 6 illustrates the relationship between drop height and relative density. In this study, the terminal drop height of the sample was set at 34 cm, achieving a relative density of approximately 73% (Table 3), which classifies the soil as dense.

Table 4 Laboratory Test Configurations: Single and Group Piles

	Single pile	Group piles											
Center-to-center spacing (m=(d+D)/D)	-	m=1.350			m=1.530			m=1.732			m=2.500		
Case		Case A	Case B	Case C	Case A	Case B	Case C	Case A	Case B	Case C	Case A	Case B	Case C
Number	1	3			3			3			3		
Total	13												

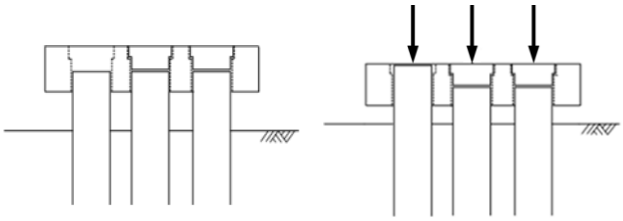

(a) Before Loading (b) After Loading

Fig. 8 Pile Settlement with Pile Cap Head Configurations

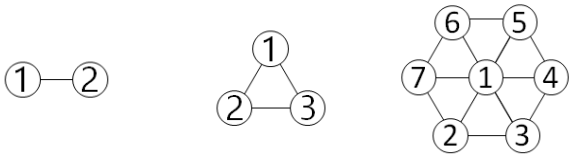

CASE A CASE B CASE C

Fig. 9 Layout of Group Piles by Arrangement

Direct Shear Test

To determine the shear resistance angle of the prepared ground, a direct shear test was conducted. By analyzing the relationship between vertical stress and shear stress, the shear resistance angle was calculated to be approximately 35° (Fig. 7). This value was used in Table 1 to calculate the pile spacing.

4.2 Laboratory model tests

This experiment was designed using the pile spacing ranges derived from the arching effect and soil wedge reinforcement interference theory. The test container was designed to be wider than the influence zone of the piles to minimize boundary effects. The model piles were fabricated from stainless steel rods with a diameter of 20 mm and a length of 250 mm. Various pile caps were also manufactured to correspond to different pile spacing ratios and used in the experiments.

The pile caps were designed with adjustable heads to control the load distribution on the group piles. Fig. 8 illustrates the settlement behavior of piles based on whether the pile cap heads were open or closed. For instance, in a configuration where only one of the three pile heads was open while the other two remained closed (a), the piles with closed heads experienced immediate settlement, whereas the open-head pile was minimally affected by the load within the predefined settlement range (b).

The test cases included group piles with 2, 3, and 7 piles, with pile spacing ratios set at 1.350, 1.530, 1.732, and 2.500. A total of 12 group pile configurations were tested, along with one single-pile case, resulting in 13 cases in total (Table 4). Figure 9 illustrates the layout of the group piles, and Figure 10 shows the setup of the pile caps.

As illustrated in Fig. 8, the test setup was designed to accommodate modifications to the group pile configuration by adjusting the pile cap heads. This approach allowed for the assessment of various group pile arrangements without the need to manufacture separate pile caps for each case.

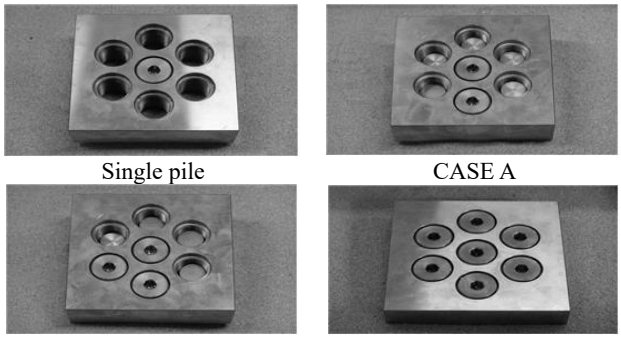

Single pile CASE A

CASE B CASE C

Fig. 10 Pile Cap Configurations: Single and Group Piles

When transitioning from Case B to Case C, the original layout was preserved, and the additional piles were symmetrically arranged. Although the 7-pile configuration in Case C is not commonly applied in practice, it was adopted to maintain symmetric load distribution under the given experimental constraints. Furthermore, this configuration enabled a stepwise increase in the number of piles while ensuring geometric consistency across cases, thereby supporting a systematic evaluation of group pile behavior. Accordingly, Case C was incorporated into the experimental program and analyzed as part of this study.

Using the terminal drop height of 34 cm determined from the sand pluviation test, the ground was compacted to maintain a consistent relative density. The drop height was set at 40 cm during soil placement using the pluviation device, ensuring a relative density of 73%. To minimize soil disturbance, the pile installation was performed concurrently with the sand pluviation process. Finally, the completed model ground was placed into the test container, and a load was applied to the top of the piles using a load cell to observe ground behavior (Fig. 11).

4.3 Laboratory model test results

The pile load tests yielded load-settlement curves, which

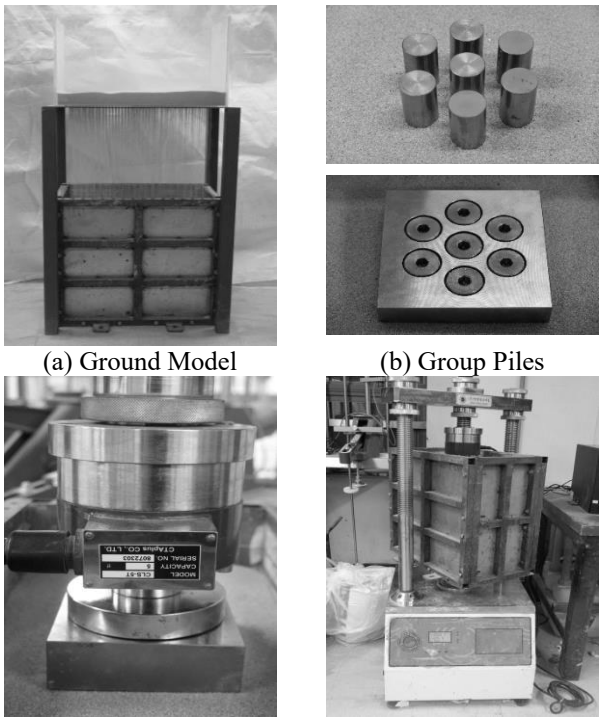

(a) Ground Model (b) Group Piles

(c) Load Cell Setup (d) Pile Loading System

Fig. 11 Static Load Test Procedure for Piles

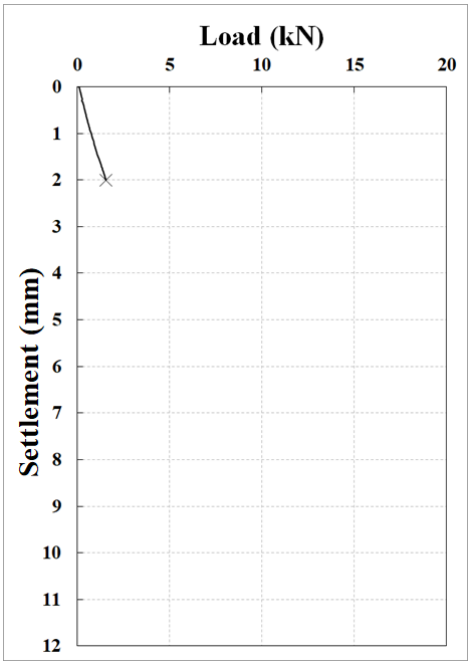

Fig 12 Load-Settlement Curve (Single)

were utilized to determine the ultimate bearing capacity. By applying BS Standards, precise soil parameters obtained from laboratory tests, such as direct shear tests, could be directly incorporated into the bearing capacity calculations. This approach enhances consistency with standardized design methodologies and ensures a more accurate reflection of actual soil behavior, resulting in more reliable estimations compared to methods relying solely on empirical formulas.

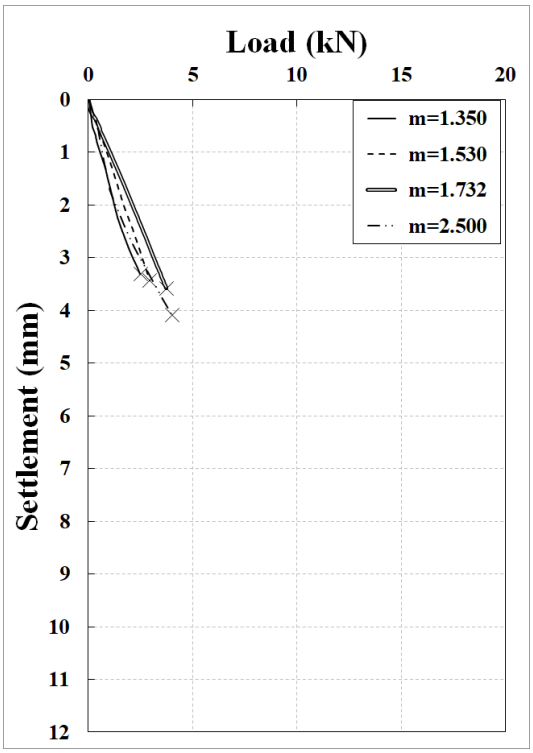

Fig. 13 Load-Settlement Curve (Case A)

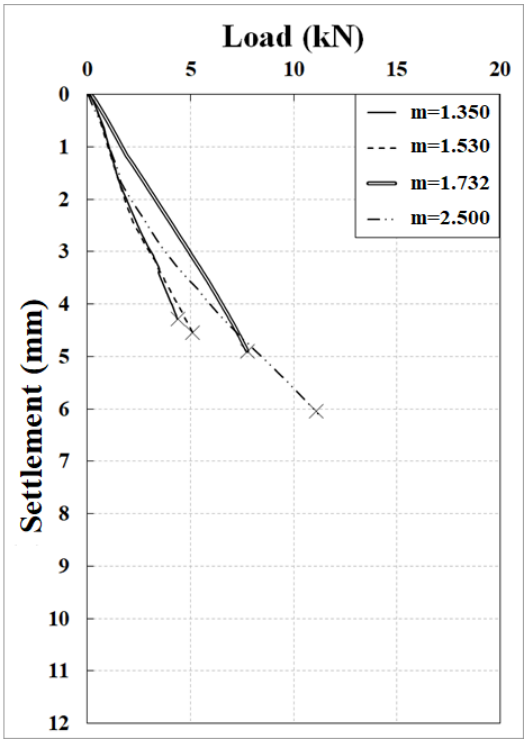

Fig. 14 Load-Settlement Curve (Case B)

The ultimate bearing capacity of driven piles and bored piles is defined as the load corresponding to a settlement of 10% and 5–10% of the pile diameter, respectively (De Beer 1988, Franke 1989). Based on these findings, this study adopted the British Standard (BS) method, defining the ultimate bearing capacity of the driven pile as the load corresponding to a settlement equal to 10% of the pile

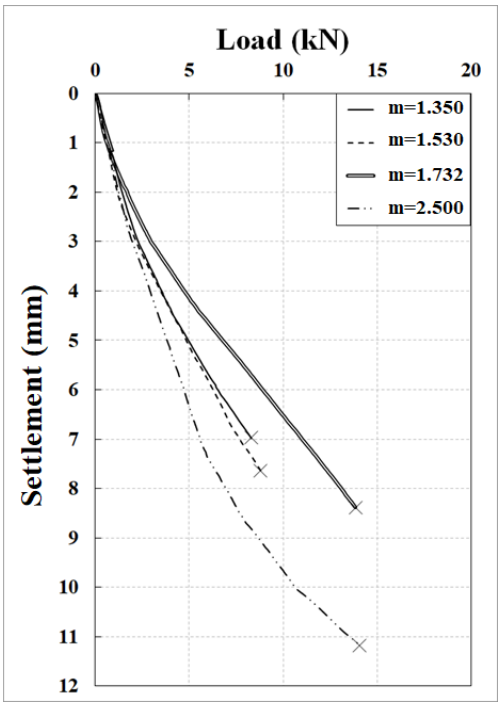

Fig. 15 Load-Settlement Curve (Case C)

Table 5 Ultimate Bearing Capacity for Single and Group Piles (Unit: kN)

	Single	Case A	Case B	Case C
m=1.350	1.797	2.549	4.358	8.325
m=1.530		2.925	5.299	8.763
m=1.732		3.719	7.710	13.825
m=2.500		4.033	11.184	14.059

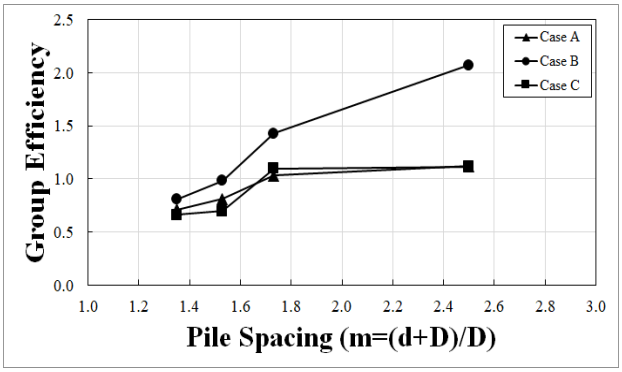

Fig. 16 Group Efficiency vs. Pile Spacing Ratio

Table 6 Group Efficiency for Different Spacing Ratios

	m=(d+D)/D	Q_{ult} (kN)	Group efficiency
Case A	1.350	2.549	0.709
	1.530	2.925	0.814
	1.732	3.719	1.035
	2.500	4.033	1.122
Case B	1.350	4.358	0.808
	1.530	5.299	0.983
	1.732	7.710	1.430
	2.500	11.184	2.075
Case C	1.350	8.325	0.662
	1.530	8.763	0.692
	1.732	13.825	1.099
	2.500	14.059	1.118

diameter. The effective diameter and ultimate bearing capacity derived from the load-settlement curves for both single and group piles are shown in Figs. 12-15.

The test results indicated that as the pile spacing increased, and as the size of the pile group grew, the ultimate bearing capacity also increased (Table 5).

An analysis of the load-settlement curves in Figs. 13-15 reveals that the slopes corresponding to the spacing ratio m exhibit irregular trends across different cases. This variation can be attributed to two primary factors. First, experimental errors, including measurement inaccuracies or limitations in equipment sensitivity, may have influenced the results. Second, the complex interaction between piles and surrounding soil must be considered, as nonlinear pile-soil behavior can contribute to deviations in the experimental data.

Although the observed slopes vary slightly between cases, such discrepancies are common in experimental studies and may result from unpredictable external factors. To ensure consistency and reliability, the BS Standard was applied in calculating the ultimate bearing capacity, providing a more systematic and structured approach to data interpretation.

The group efficiency (η) is defined as the ratio of the bearing capacity of the pile group (Q_g) to the sum of the bearing capacities of individual piles (Q_s), as expressed in Eq. (15). Here, n_1 represents the number of rows in the pile group, and n_2 represents the number of columns. The product of these values is used to calculate the sum of the individual pile capacities (Al-Mhaidib 2007).

$$\eta = \frac{Q_g}{n_1 \cdot n_2 \cdot Q_s} \tag{15}$$

Using the ultimate bearing capacities obtained from the model tests, the group efficiency was calculated. The results showed that group efficiency increased as pile spacing widened (Table 6). Notably, group efficiencies greater than 1 indicate that the group piles exhibit higher bearing capacity than the simple sum of individual piles. Fig. 16 illustrates that group efficiency exceeds 1 when the pile spacing ratio is 1.7 or greater. This finding suggests that when the pile spacing ratio exceeds 1.7, the arching effect is activated, enhancing the vertical bearing capacity of the piles.

5. Conclusions

This study analyzed the effect of pile spacing on the bearing capacity of group piles through load tests and

evaluated the changes in soil bearing capacity. The findings are summarized as follows:

- Optimal Spacing Calculation: By applying Terzaghi's pile failure mode, it was determined that the optimal spacing varies depending on the soil's shear resistance angle and relative density. This highlights the importance of considering soil characteristics when determining the optimal spacing for group piles under various ground conditions.
- Ultimate Bearing Capacity and Group Efficiency: Load tests conducted on dense sandy soil with a shear resistance angle of approximately 35° revealed that both ultimate bearing capacity and group efficiency increased as the pile spacing widened. Notably, at a spacing ratio of 1.732, the group efficiency exceeded 1, indicating that the arching effect contributes to enhanced vertical bearing capacity even at smaller spacing ratios than the current Korean design standard of a minimum 2.5D.
- Implications for Design Standards: The experimental results demonstrate that group piles can maintain high bearing capacity even at a spacing ratio of 1.732D or greater in dense sandy soil. This suggests the potential for reducing the minimum spacing required by current Korean standards (2.5D), providing a basis for more efficient pile design.

Notably, the analysis of Case B revealed the highest group efficiency at a specific spacing ratio (Fig. 16), presenting unique characteristics compared to previous studies. While prior research typically observed a gradual increase in group efficiency with wider spacing, Case B showed a peak efficiency at a specific spacing ratio (approximately 2.5D). This can likely be attributed to a combination of geometric characteristics of the pile arrangement, the activation of the arching effect, and the reinforcement from soil wedge interference.

Further investigation is required to better understand the spacing ratio that maximizes efficiency in Case B. Additional experiments and numerical analyses should focus on the interactions between pile arrangements, stress redistribution mechanisms, and the interplay between the arching effect and soil wedge reinforcement. These studies would help elucidate the mechanisms driving peak efficiency and provide concrete design guidelines, such as applying a spacing ratio range of 1.7–2.5D in practice.

Future research should also consider a wider range of soil conditions, including groundwater levels, soil strength, and density, to refine the optimal spacing further. These efforts will contribute to enhancing the efficiency of group pile designs and complement existing domestic and international design standards.

Acknowledgments

This work was supported by the National Research Foundation of Korea(NRF) grant funded by the Korea government(MSIT) (No. RS-2023-00272449).

References

AASHTO (2018), Standard specifications for highway bridges, American Association of State Highway and Transportation Officials; Washington, D.C., USA.

Abdollahi, M. and Bolouri Bazaz, J. (2017), "Reconstitution of sand specimens using a rainer system", *Int. J. Eng*., **30**(10), 1451-1463. https://doi.org/10.5829/ije.2017.30.10a.05.

Al-Mhaidib, A.I. (2007), "Efficiency of pile groups in clay under different loading rates", *Proceedings of the 17th International Offshore and Polar Engineering Conference*, Lisbon, Portugal, July.

Alsanabani, N.M., Al-Gahtani, K.S., Bin Mahmoud, A.A. and Aljadhai, S.I. (2023), "Integrated methods for selecting construction foundation type based on using a value engineering principle", *Sustainability*, **15**(11), 1-19. https://doi.org/10.3390/su15118547.

Cai, S., Huag, B., Zhao, X. and Li, J. (2023), "An application of spherical cavity expansion theory in soft rock pile-base resistance", *American Scientific Publishers*, **15**(2), 176-186, https://doi.org/10.1166/sam.2023.4408.

Dastpak, P., Abrishami, S., Anbarani, M.R. and Dastpak, A. (2021), "Effect of peforated plates on the relative density of uniformly graded reconstituted sands using air pluviation method", *Transport. Infrastruct. Geotechnol*., **8**(2), 569-589. https://doi.org/10.1007/s40515-021-00150-1.

De Beer, E. (1988), "Different behavior of bored and driven piles", *Proceedings of the 2nd International Geotechnical Seminar on Deep Foundations on Bored and Auger Piles,* W.F., Ghent, Belgium, June.

Franke, E. (1989), "CO- report to discussion, session B, on large diameter piles", *Proceedings of the 12th ICSMFE*, Rio de Janeiro, Brazil, September.

He, G., Xu, J., Jiang, J., Cao, Z. and Zhu, D. (2017), "Soil arching effect analysis and structure optimization of a robot foot sinking in soft soil", *Adv. Mech. Eng*., **9**(8), 1-9. https://doi.org/10.1177/1687814017727940.

Hong, W.P. and Hong, S.W. (2017), "Piled embankment to prevent damage to pipe buried in soft grounds undergoing lateral flow", *Mar. Georesour. Geotech*., **35**(5), 719-729. https://doi.org/10.1080/1064119X.2016.1227406.

Józefiak, K., Zbiciak, A., Maslakowski, M. and Piotrowski, T. (2015), "Numerical modelling and bearing capacity analysis of pile foundation", *Procedia Eng.*, Kraków, Poland, July.

K.G.S. (2018), "Foundation design criteria", Korean Geotechnical Society, Korean Geotechnical Society; Seoul, South Korea.

Khanmohanmmadi, M., Armaghani, D.J. and Sabri Sabri, M.M. (2022), "Prediction and optimization of pile bearing capacity considering effects of time", *Mathematics*, **10**(19), 1-15. https://doi.org/10.3390/math10193563.

KS F 2343 (2017), "Testing method for direct shear test of soil", Korean Industrial Standards, Korean Agency for Technology and Standards; Seoul, South Korea.

Kumar, S., Choudhary, S.S. and Burman, A. (2024), "Machine induced dynamic field responses of group pile with different pile arrangements", *Int. J. Geo-Eng*., **15**(1), 1-17. https://doi.org/10.1186/s40703-024-00207-3.

Lian, B., Wang, X. and Li, J. (2015), "Analysis of the soil arching effect under pile-soil coupling for a landslide in the Three Gorges Reservoir Area based on three-dimensional numerical simulation", *Proceedings of the 2015 International Conference on Mechatronics*, Electronic, Industrial and Control Engineering, Shenyang, China, April.

Lv, C.Y., Guo, Y.C. Li, Y.H. and Yao, W.M. (2023), "Experimental study on the horizontal bearing characteristics of long-short-pile composite foundation", *Int. J. Geo-Eng*., **34**(4), 341-352. https://doi.org/10.12989/gae.2023.33.4.341.

Nasrollahzadeh, E. and Hataf, N. (2019), "Experimental and numerical study on the bearing capacity of single and groups of tapered and cylindrical piles in sand", *Int. J. Geotech. Eng.*, **16**(4), 426-437. https://doi.org/10.1080/19386362.2019.1651042.

Nguyen, A.D., Nguyen, V.T. and Kim, Y.S. (2023), "Finite element analysis on dynamic behavior of sheet pile quay wall dredged and improved seaside subsoil using cement deep mixing", *Int. J. Geo-Eng.*, **23**(1), 1-18. https://doi.org/10.1186/s40703-023-00186-x.

SPS-F KOCED 0005-7383 (2019), "Test method of sand pluviation for sandy soil model", Standard for Pluviation System, KOCED Collaboratory Management Institute; Daejeon, South Korea.

Xu, Q., Xie, J., Lu, L., Wang, Y., Wu, C. and Meng, Q. (2023), "Numerical and theoretical analysis on soil arching effect of prefabricated piles as deep foundation pit supports", *Undergr. Sp.*, **16**(12), 314-330, https://doi.org/10.1016/j.undsp.2023.09.011.

Yun, J. and Han, J. (2023), "Evaluation of the effect of rubble mound on pile through dynamic centrifuge model tests", *Int. J. Geo-Eng.*, **33**(4), 415-425. https://doi.org/10.12989/gae.2023.33.4.415.

Zhang, Q.Q., Feng, R.F., Yu, Y.L., Liu, S.W. and Qian, J.G. (2019), "Simplified approach for prediction of nonlinear response of bored pile embedded in sand", *Soils Found.*, **59**(5), 1562-1578. https://doi.org/10.1016/j.sandf.2019.07.011.

Zhou, Y. and Tokimatsu, K. (2018), "Numerical evaluation of pile group effect of a composite group", *Soils Found.*, **58**(4), 1059-1067. https://doi.org/10.1016/j.sandf.2018.04.004.